

# Simulation of laser-Compton cooling of electron beams for future linear colliders

T. Ohgaki<sup>1,2</sup> and I. Endo<sup>3</sup>

<sup>1</sup> Lawrence Berkeley National Laboratory Berkeley, California 94720, USA

<sup>2</sup> Venture Business Laboratory, Hiroshima University,  
2-313 Kagamiyama, Higashi-Hiroshima 739-8527, Japan

<sup>3</sup> Graduate School of Advanced Sciences of Matter, Hiroshima University,  
1-3-1 Kagamiyama, Higashi-Hiroshima 739-8530, Japan

(Dated: September 25, 2001)

## Abstract

We study a method of laser-Compton cooling of electron beams for future linear colliders. Using a Monte Carlo code, we evaluate the effects of the laser-electron interaction for transverse cooling. The optics with and without chromatic correction for the cooling are examined. The laser-Compton cooling for JLC/NLC at  $E_0 = 2 \text{ GeV}$  is considered.

PACS numbers: 41.75.Fr, 29.17.+w, 41.85.Gy, 13.88.+e

## I. INTRODUCTION

An operation of the  $e^+e^-$  linear collider at a center-of-mass energy of 5 TeV beyond the Large Hadron Collider and the 500 GeV  $e^+e^-$  linear collider, requires a luminosity of  $10^{35} \text{ cm}^{-2} \text{ s}^{-1}$  for a study of particle physics. To achieve the required luminosity in several TeV colliders, the phase space of the electron and positron beams must be significantly reduced before the beam is accelerated in a main linear accelerator.

The technique which could accomplish the required cooling for the linear colliders was proposed by R. Palmer and V. Telnov [1, 2] and is laser-Compton cooling. In laser-Compton cooling, the beam loses both transverse and longitudinal momentum by Compton scattered photons, during head-on collisions with laser photons. The longitudinal momentum is restored to the beam in a linear accelerator. Since the Compton scattered photons follow the initial electron trajectory with a small additional spread due to much lower energy of photons (a few eV) than the energy of electrons (several GeV), the transverse distribution of electron beams remains almost unchanged and also the angular spread is almost constant. Consequently the emittance  $\epsilon_i = \epsilon_i^0$  remains almost unchanged ( $i = x, y$ ), where  $\epsilon_i^0$  the transverse beam size and the angular divergence. At the same time, the electron energy decreases from  $E_0$  to  $E_f$ . Thus the normalized emittances have decreased as follows

$$\epsilon_n = \epsilon_n^0 \left( \frac{E_f}{E_0} \right) = \epsilon_n^0 C; \quad (1)$$

where  $\epsilon_n^0, \epsilon_n$  are the initial and final normalized emittances,  $C = E_f/E_0$ ,  $m_e$  is electron mass, and the factor of the emittance reduction  $C = E_f/E_0$ . The method of electron beam cooling, repeated many times, allows further reduction of the transverse emittances after damping rings or guns by 1-3 orders of magnitude [2].

In this paper, we have evaluated the effects of the laser-Compton interaction for transverse cooling using the Monte Carlo code [3, 4]. The simulation calculates the effects of the nonlinear Compton scattering between the laser photons and the electrons during a multi-cooling stage. Next, we examine the optics for cooling with and without chromatic correction. The laser-Compton cooling for JLC/NLC [5] at  $E_0 = 2 \text{ GeV}$  is considered in section 4. A summary of conclusion is given in section 5.

## II. LASER-ELECTRON INTERACTION

### A. Laser-Electron Interaction

TABLE I: Parameters of the electron beams for laser-Compton cooling. The value in the parentheses is given by Telnov's formulas.

$E_0$ (GeV)	$E_f$ (GeV)	C	$n_x = n_y$ (mrad)	$x = y$ (mm)	$z$ (mm)	(%)
2	0.2	10	$7.4 \cdot 10^{-8} = 2.9 \cdot 10^{-8}$	4/4	0.5	11 (9.8)
5	1	5	$3.0 \cdot 10^{-6} = 3.0 \cdot 10^{-6}$	0.1/0.1	0.2	19 (19)

In this section we describe the main parameters for laser-Compton cooling of electron beams. A laser photon of energy  $\hbar\omega_L$  (wavelength  $\lambda_L$ ) is backward-Compton scattered by an electron beam of energy  $E_0$  in the interaction point (IP). The kinematics of Compton scattering is characterized by the dimensionless parameter [2]

$$x_0 = \frac{4E_0\hbar\omega_L}{m_e^2c^4} = 0.019 \frac{E_0 [\text{GeV}]}{\lambda_L [\text{m}]}: \quad (2)$$

The parameters of the electron and laser beams for laser-Compton cooling are listed in Table I and II. The parameters of the electron beam with 2 GeV are given for JLC/NLC case in section 4. The parameters of that with 5 GeV are used for simulation in the next subsection. The wavelength of laser is assumed to be 0.5  $\mu\text{m}$ . The parameters of  $x_0$  with the electron energies 2 GeV and 5 GeV are 0.076 and 0.19, respectively.

The required laser push energy with  $Z_R = 1/\lambda_e$  is [2]

$$A = 25 \frac{\lambda_e [\text{nm}]}{E_0 [\text{GeV}]} (C = 1) [\text{J}]; \quad (3)$$

where  $Z_R = 1/(\lambda_L/\lambda_e)$ , and  $\lambda_e = 2/z$  are the Rayleigh length of laser, and the bunch lengths of laser and electron beams. From this formula, the parameters of A with the electron energies 2 GeV and 5 GeV are 56 J and 4 J, respectively.

The nonlinear parameter of laser field is [2]

$$^2 = 43 \frac{\lambda_L^2 [\text{m}^2]}{\lambda_e [\text{nm}] E_0 [\text{GeV}]} (C = 1): \quad (4)$$

In this study, for the electron energies 2 GeV and 5 GeV, the parameters of  $\lambda_e$  are 2.2 and 1.5, respectively.

The rms energy of the electron beam after Compton scattering is [2]

$$\sigma_e = \frac{1}{C^2} \left( \frac{h}{2} \sigma_{e0}^2 [\text{GeV}^2] + 0.7x_0 (1 + 0.45 C) (C - 1) E_0^2 [\text{GeV}^2] \right)^{i_1=2} [\text{GeV}]; \quad (5)$$

where the rms energy of the initial beam is  $\sigma_{e0}$  and the ratio of energy spread is defined as  $\sigma_e = \sigma_e / E_f$ . If the parameter  $x_0$  or  $\sigma_{e0}$  is larger, the energy spread after Compton scattering is increasing and it is the origin of the emittance growth in the defocusing optics, reacceleration linac, and focusing optics. The energy spreads for the electron energies 2 GeV and 5 GeV are 9.8% and 19%, respectively.

TABLE II: Parameters of the laser beams for laser-Compton cooling. The value in the parentheses is given by Telnov's formulas.

$E_0$ (GeV)	$L$ (m)	$x_0$	$A$ (J)	$R_{L,x}=R_{L,y}$ (mm)	$L_z$ (mm)	
2	0.5	0.076	300 (56)	2.1 (2.2)	0.3/0.3	1.25
5	0.5	0.19	20 (4)	1.5 (1.5)	0.1/0.1	0.4

The equilibrium emittances due to Compton scattering are [2]

$$\epsilon_{i,\text{min}} = \frac{7.2 \cdot 10^{-10} \beta_i [\text{m}]}{L [\text{m}]} \quad (i = x, y) [\text{m rad}]; \quad (6)$$

where  $\beta_i$  are the beta functions at IP. From this formula we can see that small beta gives small emittance. However the large change of the beta functions between the magnet and the IP causes the emittance growth. Taking no account of the emittance growth, for the electron energies 2 GeV and 5 GeV, the equilibrium emittances are  $5.8 \cdot 10^{-9} \text{ m rad}$  and  $1.4 \cdot 10^{-10} \text{ m rad}$ , respectively. The equilibrium emittances depended on  $\beta$  in the case  $\beta = 1$  were calculated in Ref. [2].

## B. Simulation of Laser-Electron Interaction

For the simulation of laser-electron interaction, the electron beam is simply assumed to be a round beam in the case of  $E_0 = 5 \text{ GeV}$  and  $C = 5$ . Taking no account of the emittance growth of optics, the one stage for cooling consists two parts as follows:

1. The laser-Compton interaction between the electron and laser beams.
2. The reacceleration of electrons in the linac.

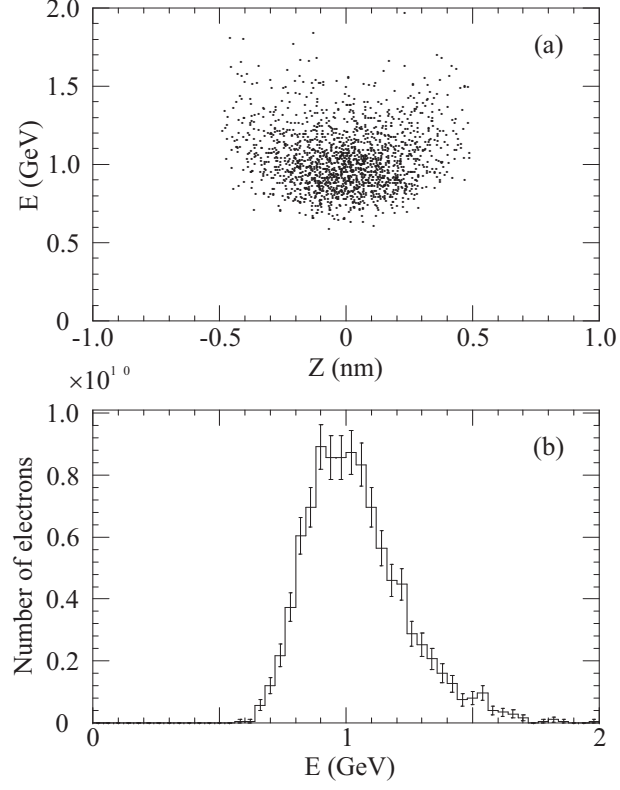


FIG . 1: The longitudinal distribution of the electrons. (a) The energy vs.  $z$ : (b) The energy distribution of the electrons. The bin size is 40 MeV .

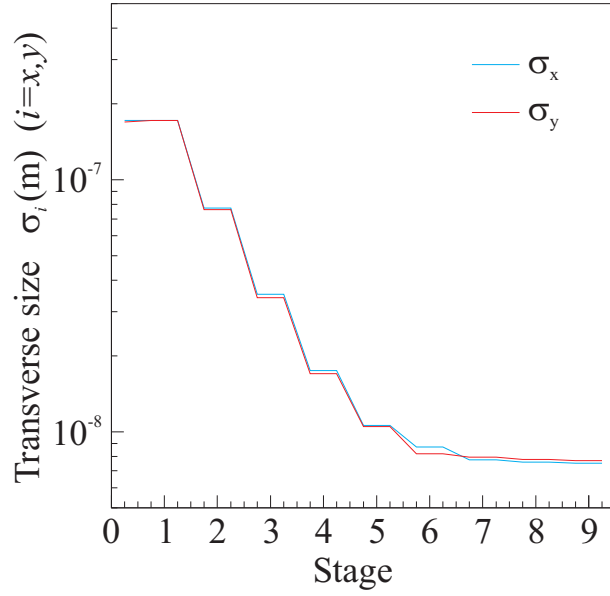


FIG . 2: The transverse sizes of the electron beams.

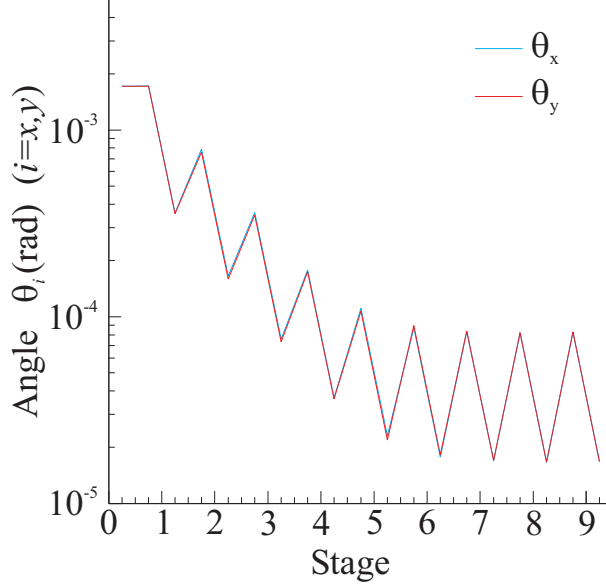


FIG. 3: The angles of the electron beams.

In the first part, we simulated the interactions by the CAIN code [4]. This simulation calculates the effects of the nonlinear Compton scattering between the laser photons and the electrons. We assumed that the laser pulse interacts with the electron bunch in head-on collisions. The  $x_0$  and  $y_0$  at the IP are fixed to be 0.1 mm. The initial energy spread of the electron beams is 1%. The energy of laser pulse is 20 J. The polarization of the electron and laser beams are  $P_e = 1.0$  and  $P_L = 1.0$  (circular polarization), respectively. When the  $x_0$  parameter is small, the spectrum of the scattered photons does not largely depend on the polarization combination. In order to accelerate the electron beams to 5 GeV for recovery of energy in the second part, we simply added the energy  $E = 5 \text{ GeV} - E_{\text{ave}}$  for reacceleration, where  $E_{\text{ave}}$  is the average energy of the scattered electron beams after the laser-Compton interaction.

Figure 1 shows the longitudinal distribution of the electrons after the first laser-Compton scattering. The average energy of the electron beams is 1.0 GeV and the energy spread is 0.19. The longitudinal distribution seems to be a bunching. If we assume a short Rayleigh length of laser pulse, the energy loss of head and tail of beams is small. The number of the scattered photons per incoming particle and the photon energy at the first stage are 40 and 96 MeV (rms energy 140 MeV), respectively.

The transverse sizes of the electron beams in the multi-stage cooling are shown in Fig. 2. During collisions with the laser photons, the transverse distribution of the electrons remains

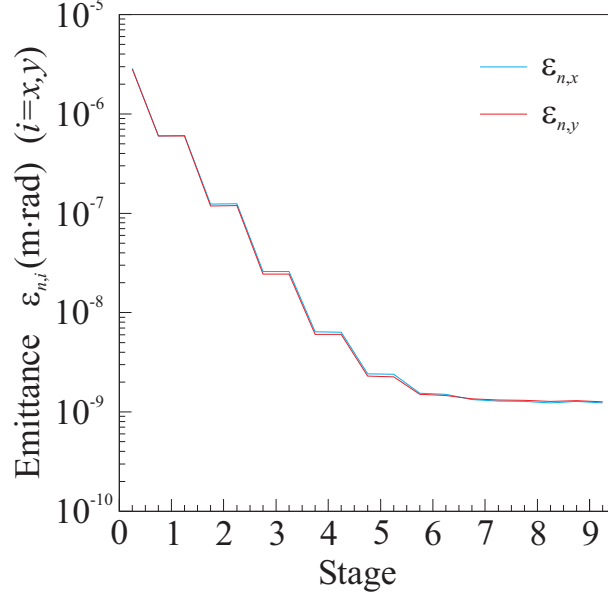


FIG . 4: The transverse emittances of the electron beams.

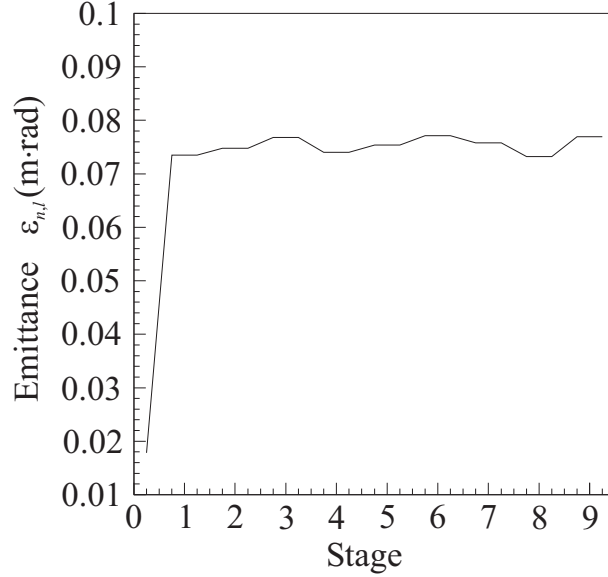


FIG . 5: The longitudinal emittance of the electron beams.

almost unchanged. But they decrease when we focus them for the next laser-Compton interaction due to the lower normalized emittance and the fixed  $\beta$ -function at IP ( $\epsilon_{n,i} = q \frac{\epsilon_{n,i}}{h_{s,i}^2}$ ). The angles of the electron beams in the multi-stage cooling,  $\epsilon_{n,i} = q \frac{\epsilon_{n,i}}{h_{s,i}^2}$  where  $h_{s,i}$  is the scattering angle of the electron, are shown in Fig. 3. As a result of reacceleration, the angles of the electrons decrease. They increase when we focus them for the next laser-Compton interaction. Finally the angles attain the average of Compton scattering angle

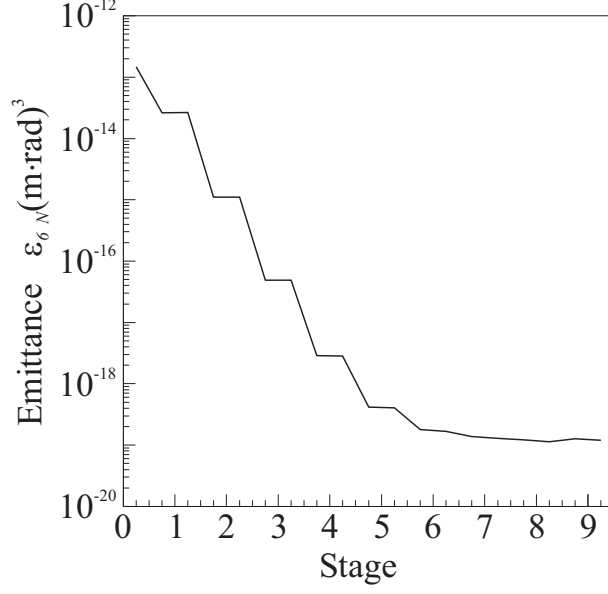


FIG .6: The 6D emittance of the electron beams.

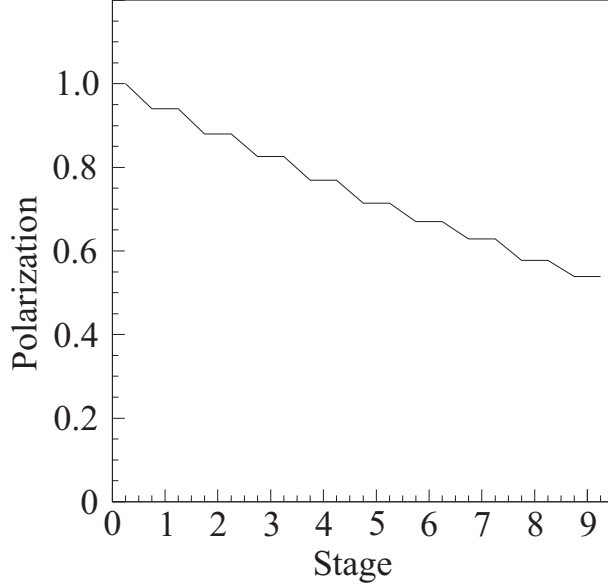


FIG .7: The polarization of the electron beams.

and the effect of cooling saturates.

Figure 4 shows the transverse emittances of the electron beams in the multi-stage cooling. From Eq.(6),  $\epsilon_{\text{min}} = 1.4 \times 10^{-10} \text{ m·rad}$ , and the simulation presents  $\epsilon_{\text{min}} = 1.2 \times 10^{-9} \text{ m·rad}$ . Figure 5 shows the longitudinal emittance of the electron beams in the multi-stage cooling. Due to the increase of the energy spread of the electron beams from 1% to 19%, the longitudinal emittance rapidly increases at the first stage. After the first stage, the



normalized longitudinal emittance is stable. The 6D emittance of the electron beams in the multi-stage cooling is shown in Fig. 6. The second cooling stage has the largest reduction for cooling. The 8th or 9th cooling stages have small reduction for cooling. The initial and final 6D emittances  $\epsilon_{6N}$  are  $1.5 \times 10^{13}$  (m rad) and  $1.2 \times 10^{19}$  (m rad), respectively.

Figure 7 shows the polarization of the electron beams in the multi-stage cooling. The decrease of the polarization during the first stage is about 0.06. The final polarization  $P$  after the multi-stage cooling is 0.54.

### III. OPTICS DESIGN FOR LASER-COMPTON COOLING

#### A. Optics without chromaticity correction

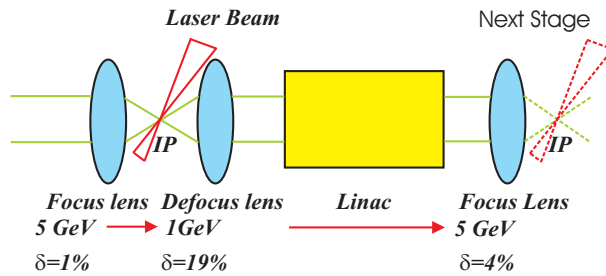


FIG. 8: Schematic diagram of the laser-Compton cooling of the electron beams.

There are three optical devices for the laser-Compton cooling of electron beams as follows:

1. The focus optics to the first IP.
2. The defocus optics from the first IP to the reacceleration linac.
3. The focus optics from the linac to the next IP.

Figure 8 shows a schematic diagram of the laser-Compton cooling of the electron beams. The optics 1 is focusing the electron beams from a few meters of defocus to several millimeters in order to effectively interact them with the laser beams. The optics 2 is defocusing them from several millimeters to a few meters for reacceleration of electron beams in a linac. In a multi-stage cooling system, the optics 3 is needed for cooling in the next stage. The key problem for the focus and defocus optical devices is the energy spread of electrons and the

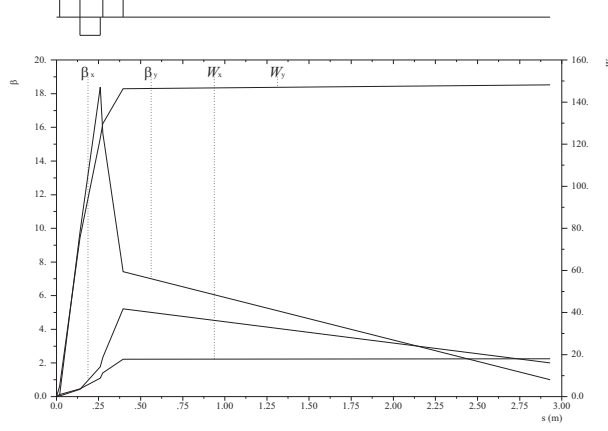


FIG . 9: The defocus optics without chromaticity correction for laser-Compton cooling.

electron beam with a large energy spread are necessary to minimize or correct the chromatic aberrations avoiding emittance growth.

In this subsection we discuss the optics for laser-Compton cooling without chromatic corrections. For the focus and defocus of the beams, we use the normal doublet system which is similar to that of the normal focus system of the future linear colliders [5]. The pole-tip field of the normal quadrupole  $B_T$  is limited to 1.2 T and the pole-tip radius  $a$  is greater than 3 mm. The strength of the normal quadrupole is

$$k = B_T = (aB) = 120E [\text{GeV}] [\text{m}^{-2}]; \quad (7)$$

where  $B$ ,  $a$ , and  $E$  are the magnetic field, the radius of curvature, and the energy of the electron beams. In our case, the electron energies in the optics 1, 2, and 3 are 5.0, 1.0, and 5.0 GeV, respectively and the limit of the strength of the quadrupole in laser cooling is much larger than that of the normal quadrupole of the future linear colliders. Due to the low energy beams in laser cooling, the synchrotron radiation from quadrupoles and bends is negligible.

The difference of three optical devices is the amount of the energy spread of the beams. In the optics 1, 2, and 3, the beams have one, several tens, and a few % energy spread. In order to minimize the chromatic aberrations, we need to shorten the length between the normal quadrupole and the IP. In this study, the length from the face of the normal quadrupole to the IP,  $l$  is assumed to be 2 cm. Here we estimated the emittance growth in the optics 2, because the chromatic effect in the optics 2 is the most serious. Figure 9 shows the defocus optics for laser-Compton cooling by the MAD code [6]. The input file is attached to Ref. [7]. The parameters of the electron beam for laser-Compton cooling at  $E_0 = 5 \text{ GeV}$  and  $C = 5$

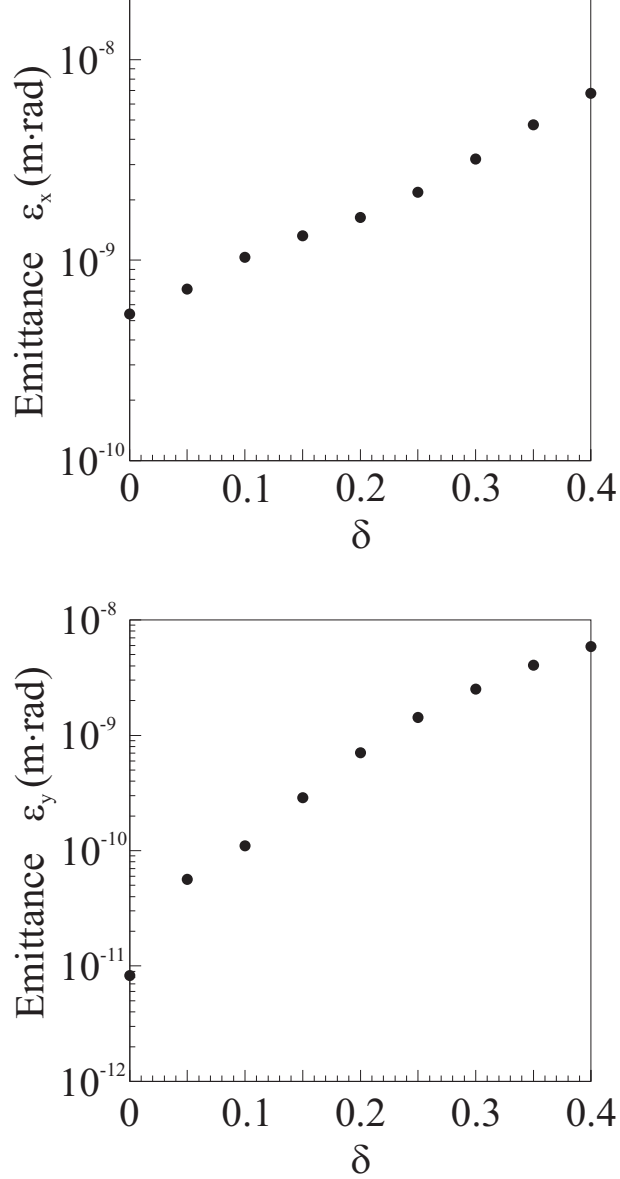


FIG. 10: Momentum dependence of the emittances in the defocus optics without chromaticity correction.

are listed in Table III. The initial  $x$  and  $y$  after laser-Compton interaction are 20 mm and 4 mm, respectively. The initial  $x$  and  $y$  are assumed to be 2 m and 1 m, respectively. The initial and final  $x(y)$  with no energy spread  $= 0$  are 0 in this optics. The strength of the final quadrupole for the beam energy of 1 GeV from Eq. (7) is assumed to be 120 m<sup>-2</sup>.

In our case, the chromatic functions  $x$  and  $y$  are 18 and 148, respectively. The momentum dependence of the emittances in the defocus optics without chromaticity correction is shown in Fig. 10. In the paper [8], the analytical study by thin-lens approximation has

TABLE III: Parameters of the electron beam for laser-Compton cooling at  $E_0 = 5 \text{ GeV}$  and  $C = 5$  for the optics design.

$E_0 \text{ (GeV)}$	$\sigma_x = \sigma_y \text{ (m rad)}$	$\sigma_x = \sigma_y \text{ (mm)}$	$\sigma_x = \sigma_y \text{ (m)}$	$\sigma_z \text{ (mm)}$
5	$1.06 \cdot 10^{-6} = 1.6 \cdot 10^{-8}$	20/4	$3.3 \cdot 10^{-5} = 1.8 \cdot 10^{-7}$	0.2

been studied for the focusing system, and here the transverse emittances are calculated by a particle-tracking simulation. The 10000 particles are tracked for the transverse and longitudinal Gaussian distribution by the MAD code. The relative energy spread is changed from 0 to 0.4. Due to the larger chromaticity  $\chi_y$ , the emittance  $\epsilon_y$  is rapidly increasing with the energy spread. If we set a limit of 200% for  $\epsilon_i = \epsilon_i$  ( $i = x, y$ ), the permissible energy spread  $\epsilon_x$  and  $\epsilon_y$  are 0.11 and 0.012 which mean the momentum bandwidth 22% and 2.4%, respectively. The results are not sufficient for cooling at  $E_0 = 5 \text{ GeV}$  and  $C = 5$ , because the beams through the defocusing optics have the energy spread of several tens %. On the one hand, the optics can be useful as the optics 1 and 3 with the energy spread of a few %.

#### B. Optics with chromaticity correction

The optics without chromaticity correction for the optics 2 does not work as we seen before subsection. In this subsection we apply the chromaticity correction for the optics 2. The lattice for cooling is designed referring to the final focus system of the future linear colliders by K. Oide [9]. The final doublet system is the same lattice as the optics before subsection. The method of chromaticity correction uses one family of sextupole to correct for vertical chromaticity and moreover we added two weak sextupoles in the lattice to correct for horizontal chromaticity. Figure 11 shows the defocus optics with chromaticity correction for laser-Compton cooling. The input file is attached to Ref. [7]. The total length of the lattice is about 63 m.

The momentum dependence of the emittances in the defocus optics with chromaticity correction is shown in Fig. 12. The 10000 particles are tracked for the transverse and longitudinal Gaussian distribution by the MAD code. The relative energy spread is changed from 0 to 0.06 with the conservation  $\epsilon_2 B$ , where  $\epsilon_2$  and  $B$  are the strength of the sextupole

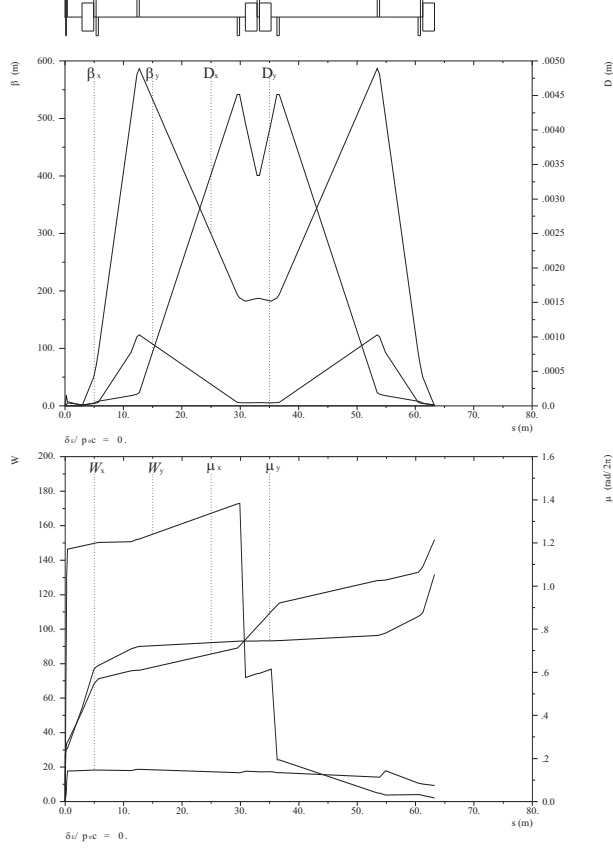


FIG . 11: The defocus optics with chromaticity correction for laser-Compton cooling.

and the angle of the bending magnet. The initial  $x$  and  $y$  after laser-Compton interaction are 20 mm and 4 mm, respectively. The initial  $x$  and  $y$  are assumed to be 2 m and 1 m, respectively. The initial and final  $x$  ( $y$ ) with no energy spread  $\delta = 0$  are 0 in this optics. After the chromaticity correction, the chromaticity functions  $x$  and  $y$  are 9.3 and 1.6, respectively. If we set a limit of 200% for  $\delta_i = \delta_i$  ( $i = x; y$ ), the permissible energy spread  $x$  and  $y$  are 0.040 and 0.023 which mean the momentum bandwidth 8% and 4.6%, respectively. By the comparison with the results of the optics with chromaticity correction at a limit of 200% for  $\delta_i = \delta_i$  ( $i = x; y$ ), the  $y$  of the optics without chromaticity correction is about two times larger than that of the one with chromaticity correction, but the  $x$  of the optics with chromaticity correction is three times smaller than that of the one before. The results are still not sufficient for cooling with  $E_0 = 5$  GeV and  $C = 5$ . These results emphasize the need to pursue further ideas for plasma lens [10].

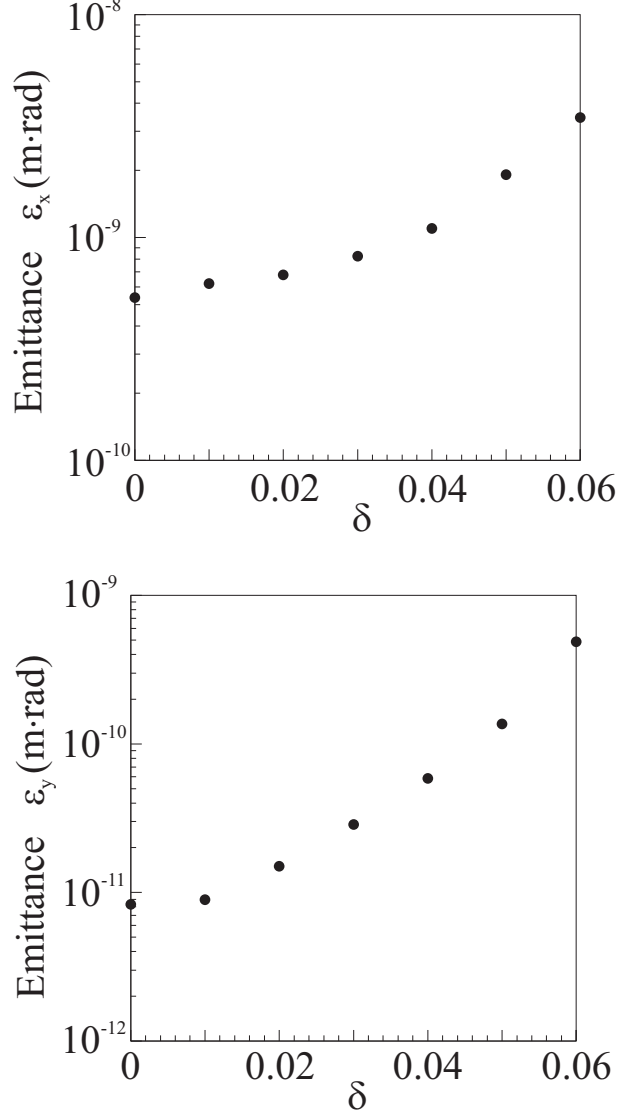


FIG. 12: Momentum dependence of the emittances in the defocus optics with chromaticity correction.

#### IV. LASER-COMPTON COOLING FOR JLC/NLC AT $E_0 = 2 \text{ GeV}$

##### A. Optics without chromaticity correction

For the future linear colliders, the method of laser-Compton cooling is effective to reduce the transverse emittances after damping rings. Where can it be placed? There are two possibilities for JLC/NLC [11] as follows:

1. After the first bunch compressor (BC1) and before the pre-linac.  $E_0 = 2 \text{ GeV}$  and  $\sigma_z = 0.5 \text{ mm}$ .

2. After the second compressor (BC2) and before the main linac.  $E_0 = 10$  GeV and  $\sigma_z = 0.1$  mm.

The case 2 needs a large energy for recovery after Compton scattering and we consider the case 1 in this study. The parameters of the electron and laser beams for laser-Compton cooling for JLC/NLC at  $E_0 = 2$  GeV and  $C = 10$  are listed in Table I and II. The energy of laser pulse is 300 J. The simulation results of the laser-electron interaction by the CAIN code are summarized as follows. The energy spread of the electron beam is 11%. The decrease of the longitudinal polarization of the electron beam is 0.038 ( $P_e = 1.0; P_L = 1.0$ ). The number of the scattered photons per incoming particle and the photon energy are 200 and 8.9 MeV (rms energy 19 MeV), respectively.

TABLE IV : Parameters of the defocus optics for laser-Compton cooling for JLC/NLC at  $E_0 = 2$  GeV and  $C = 10$ .

l	Length of Q1	Field of Q1	Aperture	Total length
5 mm	2 cm	1.2 Tesla	0.5 mm	7.4 cm

The electron energy after Compton scattering in the case 2 is 0.2 GeV and the strength of the normal quadrupole from Eq. (7) is  $600 \text{ m}^{-2}$ . Table IV lists the parameters of the defocusing optics for laser-Compton cooling for JLC/NLC at  $E_0 = 2$  GeV and  $C = 10$ . The  $\sigma_x$  and  $\sigma_y$  are assumed to be 1 mm and 0.25 mm, respectively. The chromaticity functions  $\chi_x$  and  $\chi_y$  are 18 and 23, respectively. Using the MAD code, the emittance growth in the defocus optics is

$$\epsilon_{nx}^{\text{defocus}} = \epsilon_{nx} - \epsilon_{nx0} = 1.0 \epsilon_{nx0} = 7.6 \times 10^8 \text{ [m}^2 \text{ rad]}; \quad (8)$$

$$\epsilon_{ny}^{\text{defocus}} = \epsilon_{ny} - \epsilon_{ny0} = 1.6 \epsilon_{ny0} = 4.6 \times 10^8 \text{ [m}^2 \text{ rad]}; \quad (9)$$

where the normalized emittances before and after the defocus optics are  $\epsilon_{ni0}$  and  $\epsilon_{ni}$  ( $i = x, y$ ), respectively. The emittance growth in the other two-focus optics is negligible.

## B. Reacceleration Linac

In the reacceleration linac, there are two major sources of the emittance increase [11] as follows:

1. The emittance growth due to the misalignment of the quadrupole magnet and the energy spread.
2. The emittance growth due to the cavity misalignment.

The emittance growth due to these sources in the reacceleration linac is formulated by K. Yokoya [11]

$$\frac{\text{linac}}{n_x} = 0.32_{n_x0} \quad 2.4 \quad 10^8 \text{ [m rad]}; \quad (10)$$

$$\frac{\text{linac}}{n_y} = 0.32_{n_y0} \quad 2.4 \quad 10^8 \text{ [m rad]}; \quad (11)$$

The natural emittance growth and the natural emittance with  $C = 10$  are

$$n_x = 1.3_{n_x0} \quad 1.0 \quad 10^7 \text{ [m rad]} \rightarrow n_x = 0.23_{n_x0}; \quad (12)$$

$$n_y = 2.4_{n_y0} \quad 7.0 \quad 10^8 \text{ [m rad]} \rightarrow n_y = 0.34_{n_y0}; \quad (13)$$

The total reduction factor of the 6D emittance of the laser-Compton cooling for JLC/NLC at  $E_0 = 2 \text{ GeV}$  is about 13. The decrease of the polarization of the electron beam is 0.038 due to the laser-Compton interaction.

## V. SUMMARY

We have studied the method of laser-Compton cooling of electron beams for future linear colliders. The effects of the laser-Compton interaction for cooling have been evaluated by the Monte Carlo simulation. From the simulation in the multi-stage cooling, we presented that the low emittance beams with  $\epsilon_N = 1.2 \times 10^{-19} \text{ (m rad)}$  can be achieved in our beam parameters. We also examined the optics with and without chromatic correction for cooling, but the optics are not sufficient for cooling due to the large energy spread of the electron beams.

The laser-Compton cooling for JLC/NLC at  $E_0 = 2 \text{ GeV}$  and  $C = 10$  was considered. The total reduction factor of the 6D emittance of the laser-Compton cooling is about 13. The decrease of the polarization of the electron beam is 0.038 due to the laser-Compton interaction.



## Acknowledgments

We would like to thank Y. Nosochkov, K. Oide, T. Takahashi, V. Telnov, M. Xie, and K. Yokoya for useful comments and discussions. This work was supported in part by the U.S. Department of Energy under Contract No. DE-AC03-76SF00098.

---

- [1] R. Palmer, Nucl. Instrum. and Methods Phys. Res. A 355, 150 (1994).
- [2] V. Telnov, Phys. Rev. Lett. 78, 4757 (1997); *ibid.* 80, 2747 (1998); in Proceedings of the 15th Advanced ICFA Beam Dynamics Workshop on Quantum Aspects of Beam Physics, Monterey, CA, 4-9 Jan 1998, BUDKER INP-98-33 (1998); Nucl. Instrum. and Methods Phys. Res. A 455, 80 (2000).
- [3] T. Ohgaki, The 3rd International Workshop on Electron-Electron Interactions at TeV Energies, Dec 10-12, (Santa Cruz, California) 1999, Int. J. Mod. Phys. A 15, 2587 (2000).
- [4] P. Chen, T. Ohgaki, A. Spitkovsky, T. Takahashi, and K. Yokoya, Nucl. Instrum. and Methods Phys. Res. A 397, 458 (1997).
- [5] Zeroth-Order Design Report for the Next Linear Collider, LBNL-PUB-5424, SLAC Report-474 (1996); JLC Design Study, KEK Report-97-1 (1997); Conceptual Design of a 500 GeV Electron Positron Linear Collider with Integrated X-Ray Laser Facility, DESY-97-048, ECFA-97-182 (1997).
- [6] H. Grote and F.C. Iselin, The MAD Program (Methodical Accelerator Design) Version 8.19: User's Reference Manual, CERN-SL-90-13-AP (1996).
- [7] T. Ohgaki, LBNL-44380 (1999).
- [8] B.W. Montague and F. Ruggiero, CLIC-NOTE-37 (1987).
- [9] K. Oide, Nucl. Instrum. Meth. Phys. Res. A 276, 427 (1989); in Proceedings of the DPF Summer Study on High Energy Physics in the 1990's, Snowmass, CO, Jun 27-Jul 15 1988, SLAC-PUB-4806 (1988); in Proceedings of the 1st Workshop on the Japan Linear Collider (JLC), Tsukuba, Japan, Oct 24-25, 1989, KEK Preprint-89-190 (1989).
- [10] P. Chen, K. Oide, A.M. Sessler, and S.S. Yu, Phys. Rev. Lett. 64, 1231 (1990); in Proceedings of the Fourteenth International Conference on High Energy Accelerators, Tsukuba, Aug 22-26, 1989, SLAC-PUB-5060 (1989).

[11] K. Yokoya, Nucl. Instrum. and Methods Phys. Res. A 455, 25 (2000).